Ozonation process intensification of *p*-nitrophenol by *in situ* separation of hydroxyl radical scavengers and microbubbles

Wen Cheng, Li Jiang, Xuejun Quan, Chen Cheng, Xiaoxue Huang, Zhiliang Cheng and Lu Yang

ABSTRACT

The ozonation efficiency for removal of recalcitrant organic pollutants in alkaline wastewater is always low because of the presence of some hydroxyl radical scavengers. To solve this problem, the $O_3/Ca(OH)_2$ system was put forward, and *p*-nitrophenol (PNP) was chosen to explore the mechanism of this system. The effects of key operational parameters were studied respectively; the $Ca(OH)_2$ dosage 3 g/L, ozone inlet flow rate 3.5 L/min, ozone concentration 65 mg/L, reactor pressure 0.25 MPa, and temperature 25 °C were obtained as the optimal operating conditions. After 60 min treatment, the organic matter mineralized completely, which was higher than the sum of the ozonation-alone process (55.63%) and the $Ca(OH)_2$ process (3.53%). It suggests that the calcium hydroxide in the $O_3/Ca(OH)_2$ process possessed a paramount role in the removal of PNP. The liquid samples and the precipitated substances were analyzed by gas chromatography mass spectrometry, X-ray diffraction, scanning electron microscopy and Fourier transform infrared spectroscopy; it was demonstrated that $Ca(OH)_2$ could accelerate the generation of hydroxyl radical and simultaneously *in situ* separate partial intermediate products and CO_3^{2-} ions through some precipitation reactions.

Key words | hydroxyl radical scavenger, *in situ* separation, microbubble, ozonation, *p*-nitrophenol (PNP)

Wen Cheng
Xuejun Quan (corresponding author)
Chen Cheng
Xiaoxue Huang
Zhiliang Cheng
College of Chemistry and Chemical Engineering,
Chongqing University of Technology,
Chongqing 400054,
China
E-mail: *hengjunq@cqut.edu.cn*

Li Jiang
College of Artificial Intelligence and Big Data,
Chongqing College of Electronic Engineering,
Chongqing 401331,
China

Lu Yang
Chongqing Municipal Solid Waste Resource Utilization & Treatment Collaborative Innovation Center,
Chongqing 401331,
China

INTRODUCTION

As a green and efficient advanced oxidation process (AOP), ozonation has been considered a promising method for wastewater treatment as it is flexible in operation (Shahidi *et al.* 2015); meanwhile, it is unlimited by the colloid substance and has easy operation (Bauman *et al.* 2011; Kumar *et al.* 2017). Also, due to its strong oxidation-reduction potential, ozonation can degrade macromolecular organic matter into smaller molecules and achieve the high oxidation and decolorization efficiency (Zeng *et al.* 2012). However, several disadvantages limit its application, such as: (i) short half-life and easy decomposition, leading to the high cost (Cheng *et al.* 2016); (ii) the low reaction rate and limited mass transfer resulting from the relatively low solubility and stability in water (Izadifard *et al.* 2018); (iii) selectivity between ozone and organic molecules, hindering the ozonation process (Xiong *et al.* 2016). Therefore, it is essential to accelerate the mass transfer rate of ozone and generate the hydroxyl radical; catalytic ozonation has been investigated as an efficacious way for oxidation (Cheng *et al.* 2016).

On the one hand, the pH of the liquid media has a significant impact on the process of catalytic ozonation, which can be divided into two common aspects. Firstly, catalysts could be utilized to facilitate ozone decomposition and strengthen the formation of active radicals (Wang & Bai 2016), but it is important to keep the catalytic ozonation process in the acidic media, and that carbon dioxide as mineralized product can overflow to the reaction system, without consuming hydroxyl radicals (Nawrocki & Kasprzyk-Hordern 2010). However, the stability of catalysts should be further considered. The leaching of catalytic active components and the easy contamination of catalysts are problems that must be investigated in actual wastewater treatment (Hu *et al.* 2016). Secondly, ozone decomposition in water is greatly decided by pH in the solution and

doi: 10.2166/wst.2019.227

occurs faster when the pH value increases to 10. Basic pH is favorable for ozone decomposition; in general, the decomposition of O_3 in water is initiated by OH^- (e.g. conventional O_3/H_2O_2 process) (Yu *et al.* 2011; Asgari *et al.* 2013). Nevertheless, there are HCO_3^- and CO_3^{2-} ions that will generate in alkaline condition due to the pollutant mineralization, resulting in the consumption of hydroxyl radicals by some free radical scavengers and decline of the oxidation efficiency (Kuosa *et al.* 2015).

Calcium hydroxide is a kind of cheap and environmental-friendly chemical with a moderate solubility in water. Calcium hydroxide in aqueous solution first ionizes into calcium ions and hydroxyl ion; the pH value in solution could be maintained by $Ca(OH)_2$ to promote ozone decomposition. And then the Ca^{2+} would react with HCO_3^- and CO_3^{2-} ions; therefore, the CO_3^{2-} ions could be simultaneously precipitated and separated due to the presence of Ca^{2+} ions, resulting in high ozonation efficiency.

On the other hand, in order to improve the ozone–water mass transfer efficiency in engineering applications, many strengthening measures were explored by numerous scholars, such as an oscillatory baffled reactor (Al-Abduly *et al.* 2014), planar falling film reactor (Mahyar *et al.* 2017), and rotating packed bed reactor (Zeng *et al.* 2012). It has been reported that microbubbles can improve the gas–liquid mass transfer rate, and the ozone-microbubble in the liquid phase will generate hydroxyl radical during shrinks and burst instantaneously (Takahashi *et al.* 2012). Compared with a conventional bubble reactor, the gas–liquid mixing pump was utilized to disperse the mixture gas of oxygen and ozone into numerous micro gas bubbles with micro-scale in the microbubble reactor, realizing the compulsory mixing of ozone and wastewaters, therefore enhancing utilization of ozone and improving the mass transfer rate.

Phenols are generally considered to be one of the most important organic pollutants discharged into the environment, causing unpleasant taste and odor of drinking water (Alshehri *et al.* 2014; Al-Kahtani *et al.* 2018). *p*-Nitrophenol (PNP) is an important chemical raw material used as a typical phenolic compound to produce explosives, preservatives, pharmaceuticals, pesticides and dyes (Wang *et al.* 2015). In a typical chemical industrial organic wastewater, it is difficult to degrade. Thus, this work mainly aimed to evaluate the ozonation efficiency using PNP as a model pollutant and explore the mechanism of the O_3/$Ca(OH)_2$ process in a microbubble reactor. Effects of $Ca(OH)_2$ dosage, pressure, temperature, initial PNP concentration, ozone concentration and inlet flow rate on the degradation and mineralization of PNP are discussed respectively. Furthermore, the mechanism of PNP mineralization is discussed thoroughly through the *in situ* separation effects of $Ca(OH)_2$ towards hydroxyl radical scavengers and some ozonation intermediate products.

MATERIALS AND METHODS

Reagents

Details of reagents used in this study are provided in the Supporting information (available with the online version of this paper).

O_3/$Ca(OH)_2$ process

The experimental setup for the ozonation experiments is shown in Figure 1. More details about this setup are given elsewhere (Quan *et al.* 2017). The samples were collected at regular intervals during the ozonation process, and the solid–liquid mixture was separated. The liquid sample was used to determine the PNP concentration and total organic carbon (TOC) and the intermediate products in the id sample were analyzed by gas chromatography-mass spectrometry (GC-MS); the solid phase sample was dried at 105 °C and used for analysis by X-ray diffraction (XRD), scanning electron microscopy (SEM) and Fourier transform infrared (FTIR) spectroscopy.

Analytical methods

Details of analytical methods used in this study are provided in the Supporting information.

RESULTS AND DISCUSSION

Superiority and synergetic effect of the O_3/$Ca(OH)_2$ system and microbubbles

In order to evaluate the synergetic effect of the O_3/$Ca(OH)_2$ process and microbubbles, comparative experiments and analyses using (a) bubble–O_3, (b) microbubble–O_3, (c) $Ca(OH)_2$, (d) O_3/$Ca(OH)_2$ and (e) O_3/NaOH were set up to treat PNP solution, and the results are shown in Figure 2. A lower degradation efficiency of PNP was obtained by ozone alone in the traditional bubble rector compared to the microbubble reactor. The enhancement of the mass transfer rate and utilization of ozone in the liquid led to the high ozonation rate in the microbubble reactor.

Otherwise, for the sake of highlighting the superiority of the O_3/$Ca(OH)_2$ process, compared to the process of (b), (c),

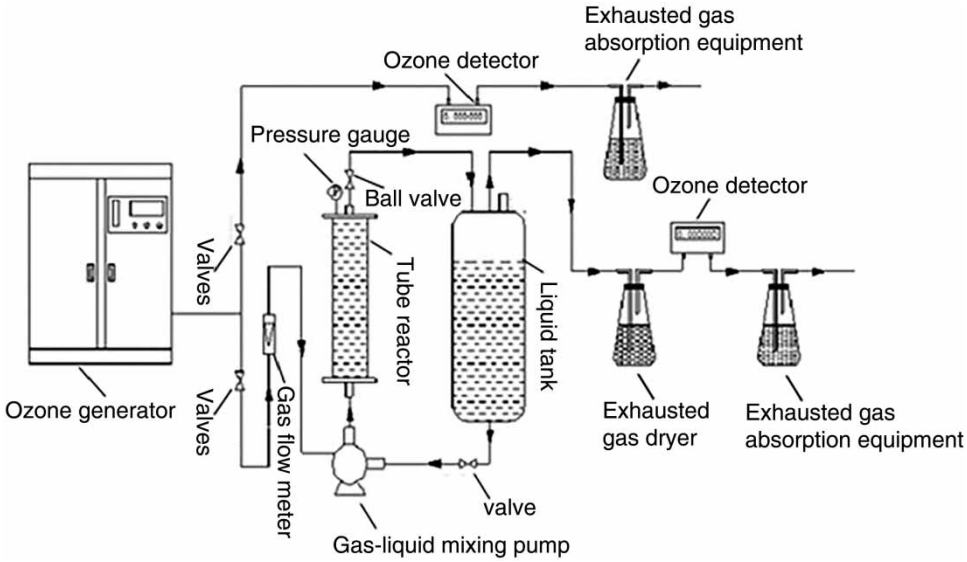

Figure 1 | Experimental setup.

(d), a high PNP removal was obtained by $O_3/Ca(OH)_2$ process, while a low mineralization rate was realized by ozonation alone. It has been reported that the O_3/OH^- process could generate hydroxyl radicals by ozone decomposition; therefore, Ca^{2+} ions and Na^+ ion were compared to verify the effect of Ca^{2+} ions in the solution. The PNP degradation rate was fast in the two O_3/OH^- processes because of the efficient decolorization rate of ozone; however, the mineralization rate in the O_3/NaOH process was far lower than that in the $O_3/Ca(OH)_2$ process, and even a little lower than that in the alone O_3 process after 40 min treatment, indicating that the free radical scavengers such as CO_3^{2-} ions or HCO_3^- ions were produced.

Bicarbonate and carbonate, as well-known hydroxyl radical scavengers, firstly can react with the ·OH and exhaust the ·OH in the solution through the following reactions (Derikvandi & Nezamzadeh-Ejhieh 2017):

$$\cdot OH + CO_3^{2-} \rightarrow OH^- + CO_3^- \cdot \quad (1)$$

$$\cdot OH + HCO_3^- \rightarrow H_2O + CO_3^- \cdot \quad (2)$$

Even though the CO_3^-· could react with the organic molecule as an oxidant, its oxidation potential ($E^0 = 1.78$ V, pH 7.0) is less than that of the hydroxyl radicals ($E^0 = 2.3$ V, pH 7.0) (Khodami & Nezamzadeh-Ejhieh 2015; Senobari & Nezamzadeh-Ejhieh 2018). Thus, there is a competitive reaction in the degradation of organic matter between the carbonate radical anion and hydroxyl radical, resulting in the low removal efficiency.

In addition, research on variation of CO_3^{2-} ions in the reaction were studied by Quan and colleagues in prior work (Quan *et al.* 2017); the results showed that the CO_3^{2-} ions concentration in the $O_3/Ca(OH)_2$ process was 13.58 mg/L after 35 min treatment, which decreased as the reaction proceeded. However, the CO_3^{2-} ions concentration in O_3/NaOH process was 229 mg/L, and there was an increasing trend as the reaction proceeded; the hydroxyl radicals were consumed greatly, resulting in the ozonation efficiency being reduced.

Meanwhile, in order to observe the reaction rate intuitively, the dynamics about the degradation and the mineralization of different systems were compared, as displayed in Figure 2(c) and 2(d). The reaction rate is related to the concentration and obeys the pseudo-first order reaction kinetics (Nezamzadeh-Ejhieh & Ghanbari-Mobarakeh 2015):

$$\ln(C_t/C_0) = -k_1 t \quad (3)$$

$$\ln(TOC_t/TOC_0) = -k_2 t \quad (4)$$

where C_t is the PNP concentration at any time (mg/L), C_0 is the initial PNP concentration, k_1 is the first-order degradation rate constant (min^{-1}), t_1 represents the degradation time, TOC_t is the TOC in the solution at any time (mg/L), TOC_0 is the initial TOC concentration, k_2 is the first-order mineralization rate constant (min^{-1}), and t_2 is the mineralization time (min).

As results show, the maximum degradation and mineralization, with the maximum reaction rate constant of 0.34795 min^{-1} and 0.12535 min^{-1} respectively, were observed in the presence of $Ca(OH)_2$. These results confirm that $O_3/Ca(OH)_2$ process enhances the ozonation efficiency and exhausts hydroxyl radical scavengers.

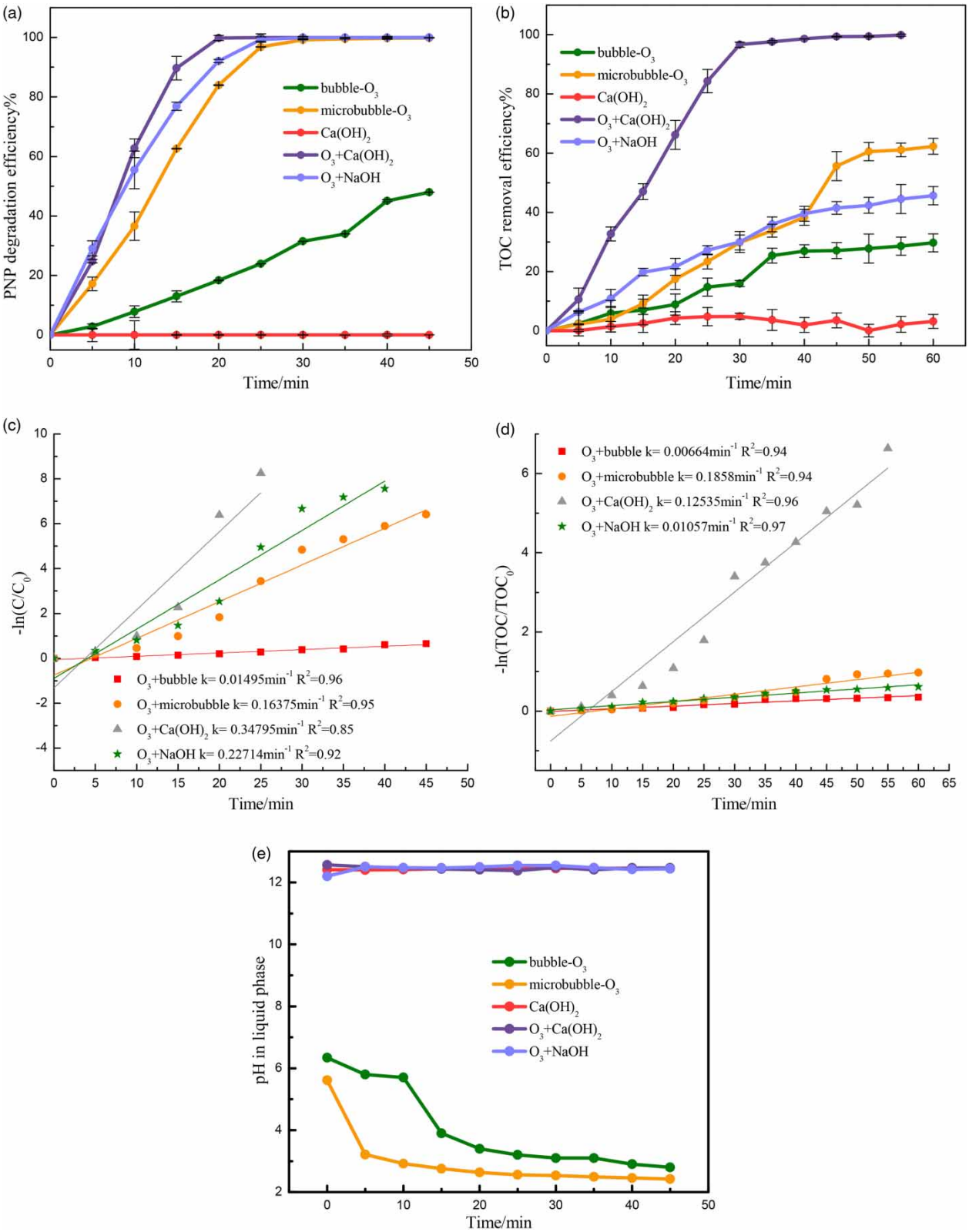

Figure 2 | Comparison of different systems: (a) bubble–O_3; (b) microbubble–O_3; (c) $Ca(OH)_2$; (d) $O_3/Ca(OH)_2$; (e) O_3/NaOH: ozone inlet flow rate 3.5 L/min; ozone inlet concentration 65 mg/L; initial PNP concentration 450 mg/L and TOC 275 mg/L; reactor pressure 0.25 MPa; $Ca(OH)_2$ dosage 3g/L; temperature 25°C.

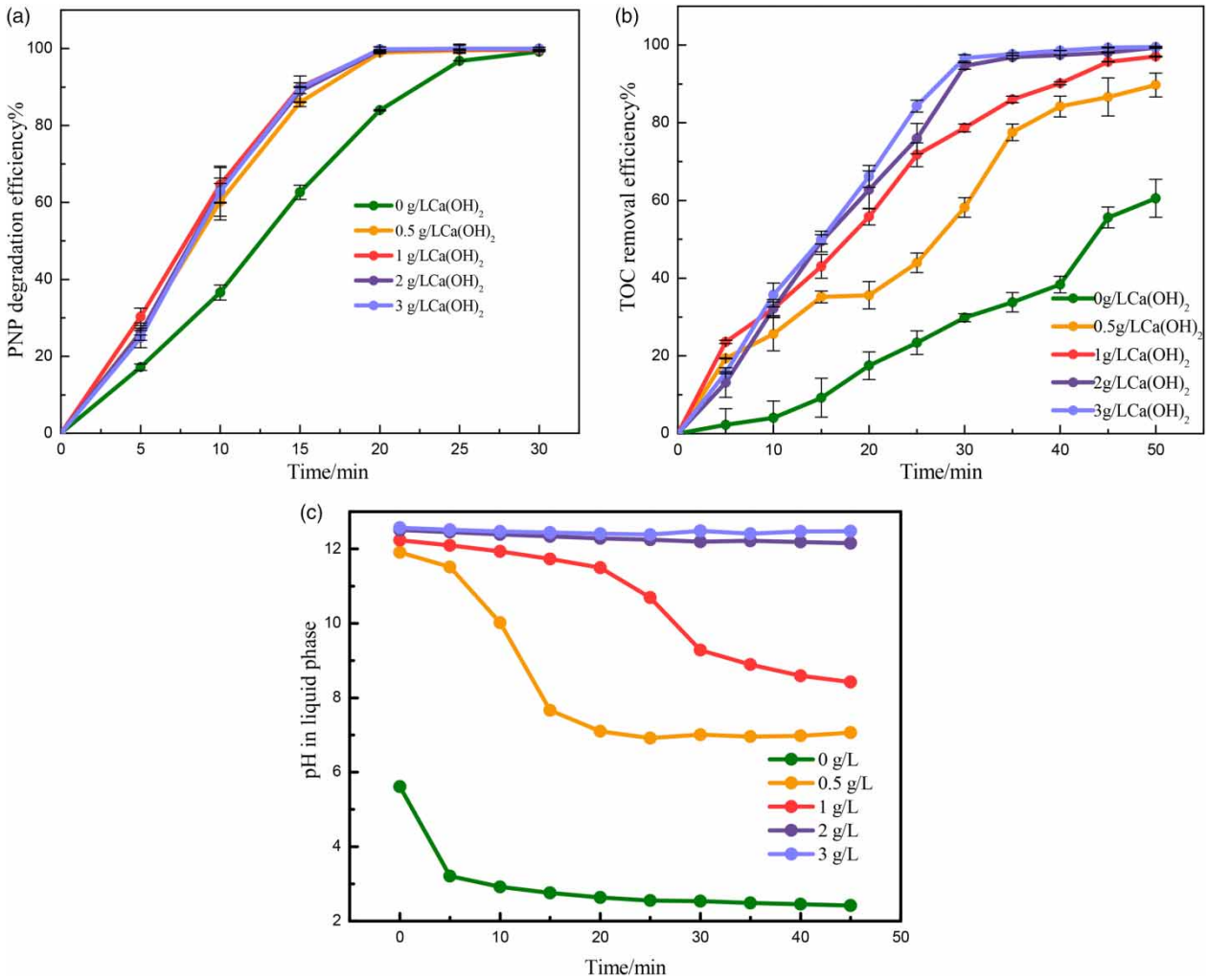

Figure 3 | Effect of $Ca(OH)_2$ dosage on removal of PNP and TOC and pH change of liquid phase: ozone inlet flow rate 3.5 L/min; ozone concentration 65 mg/L; initial PNP concentration 450 mg/L and TOC 275 mg/L; external pressure 0.25 MPa; temperature 25 °C.

Effect of operating parameters

Effect of $Ca(OH)_2$ dosage

Figure 3 shows the effects of different $Ca(OH)_2$ dosage on PNP degradation and mineralization, and the pH of the solution was monitored in ozonation process. It is noted that the $Ca(OH)_2$ has promotional effects on PNP degradation; nevertheless, varying the $Ca(OH)_2$ dosage has little influence on the PNP degradation. It may be attributed to the effect of the microbubble gas–liquid reactor, which improves the mass transfer rate between the gas phase and liquid phase, leading to the enhancement of ozonation efficiency: hence, PNP could be eliminated completely with 30 min ozonation treatment alone. For the ozone-alone process, increasing pH in the solution could enhance the degradation rate as reported by previous researches (Li *et al.* 2017). Higher initial pH is beneficial to the production of hydroxyl radicals. When $Ca(OH)_2$ dosage was 0.5 g/L, the pH in the phase decreased gradually due to the generation of a small amount organic acid, the pH value remained below 10 after 10 minutes of reaction, and the free radicals produced in the solution were sufficient for the complete degradation of PNP. Therefore, variation of the $Ca(OH)_2$ dosage has little influence on removal of PNP (Wang *et al.* 2016), so PNP could be degraded rapidly.

However, Figure 3(b) indicates that $Ca(OH)_2$ dosage had a promoting influence on mineralization: the TOC removal rate increased from 62.33% to 99.46% after 50 min treatment when $Ca(OH)_2$ dosage was increased to 3 g/L. At the same time, the reaction rate constants of the degradation and mineralization processes were calculated by the pseudo-first

order reaction kinetics equation and the results are listed in Table S1 (available with the online version of this paper). According to the results, the reaction rate constants increased with the increasing $Ca(OH)_2$ dosage. Meanwhile, Figure 3(c) shows that the pH in solution increased with increasing $Ca(OH)_2$ dosage during the process, finally, the pH value remained constant. However, the high concentration of OH^- may cause the deactivation of ·OH (Nezamzadeh-Ejhieh & Khorsandi 2010). The carbonate will generate in the high alkaline environment due to the mineralization of organic matter; this process will produce some radicals which have lower oxidation potential than ·OH, which will hinder the reaction process. Thus, the addition of $Ca(OH)_2$ has a dual function on the intensification of the ozonation process. For one thing, enough alkalinity is needed to promote the ozone decomposition and maintain the concentration of radical in solution. For another, enough Ca^{2+} ions are needed to eliminate some intermediate product and radical scavengers, and maintain the concentration of ·OH in the liquid phase. Hence, the $Ca(OH)_2$ dosage chosen was 3 g/L.

Effect of pressure

Effects of reactor pressure on the degradation and mineralization of PNP were researched as shown in Figure S1 and the reaction rate constants can be seen in Table S1 (both available online). There are some differences in the Table S1; however, it can be seen that the reactor pressure has a barely noticeable difference on degradation and mineralization of PNP from Figure S1. Generally speaking, a vigorous agitation will be generated between the gas phase and liquid phase due to the enhancement of reactor external pressure. Meanwhile, the gas–liquid mass transfer resistance decreases, resulting in an increase in ozone mass transfer. However, the gas–liquid mixer in the microbubble reactor has great superiority for dispersion of the micro gas bubbles, and it could greatly intensify the ozone mass transfer efficiency because of the effect of the internal pressure caused by micro gas bubbles. Therefore, the external pressure imposed on the reactor has little influence on the degradation of organic pollutants (Zhang *et al.* 2016).

Effect of temperature

Effects of temperature on the degradation and mineralization of PNP were investigated as shown in Figure S2 (available online) and the reaction rate constants can be seen in Table S1. From the Table S1, the results show that the reaction rate constant decreases with the increase of temperature. Research suggests that Henry's constant H_0 for ozone in the temperature range 273–333 K can be described by Equation (5) (Rischbieter *et al.* 2000):

$$\log\left(\frac{H_0}{kPa\ \ m^3\ \ mol^{-1}}\right) = 5.12 - \frac{1230}{T/K} \tag{5}$$

where T is the temperature in the process (K). It is obviously observed that low solubilities of ozone are caused by higher temperature. Generally speaking, increasing temperature will decrease the solubility of ozone and reduce the production of hydroxyl radical, leading to the ozonation efficiency decrease.

However, in the $O_3/Ca(OH)_2$ system, the ozone could decompose rapidly and generate the free radicals due to the high pH value; the enhancement of ozonation efficiency in this process is far higher than the effect of temperature. Therefore, from the macroscopic aspect, increasing the temperature has negligible influence on the organic matter removal as shown in Figure S2. As reported by Lu & Pei (2016), 25 °C is the optimal reaction temperature.

Effect of initial PNP concentration

Effects of initial concentration of PNP on the degradation and mineralization of PNP were investigated. Figure S3 (available online) shows that the degradation and mineralization decrease with increasing initial PNP concentration in solution. The degradation efficiency for initial concentration values in the first 15 min were 98.57%, 89.71%, 71.92% and 61.11% respectively, moreover, the TOC removal efficiency in the first 25 min were 96.88%, 84.31%, 62.69% and 51.63% respectively. The process of removal rate decline with increase in initial PNP concentration is due to constant ozone dosage (Wang & Bai 2016).

Effect of ozone concentration

Effects of ozone concentration on the degradation and mineralization of PNP were investigated as shown in Figure S4 (available online) and the reaction rate constants can be seen in Table S1. It can be seen from Figure S4(a) that PNP was basically degraded after 20 minutes of reaction, but it can be seen from Table S1 that the reaction rate constant k_1 increases rapidly from 0.163 min^{-1} to 0.369 min^{-1} when the concentration of ozone increases from 30 mg/L to 65 mg/L, and decreases to 0.314 min^{-1} when the concentration of ozone increases from 65 mg/L to 75 mg/L. Table S1 shows that the variation tendency of the reaction rate

constant k_2 is the same as that for k_1. Figure S4(b) shows that the TOC removal rate increased from 61.98% to 96.67% after 30 minutes of reaction when the concentration of ozone increased from 30 mg/L to 65 mg/L, while the removal rate of TOC increased slowly to 97.85% when the concentration of ozone was further increased to 75 mg/L. A potential explanation is that the ozone concentration in liquid achieves a saturation, and the organic matter was degraded by enough ozone. Therefore, it was not necessary to increase the ozone concentration to 75 mg/L.

Effect of inlet ozone flow rate

In addition, the effects of ozone flow rate on the degradation and mineralization of PNP were investigated as shown in Figure S5 (available online) and the reaction rate constants can be seen in Table S1. The variation tendency was consistent with that of the inlet ozone concentration. The increase of ozone dosage accelerates the ozonation process. However, at the same inlet ozone concentration and the same ozonation time period, with the increase of the inlet gas flow rate, the flow rate dissolved in the liquid phase increases, and the number of bubbles in the liquid phase increases. Therefore, the mass transfer efficiency increases. However, with the increase of the flow rate, the size of bubbles increases, which reduces the specific surface area. As a result, the ozone utilization rate is reduced; so increasing the inlet ozone flow rate has no obvious promotion effect.

Verification of *in situ* separation of hydroxy radical scavengers

Liquid phase analysis

The ultraviolet (UV) adsorption spectra of the wastewater before and after the $O_3/Ca(OH)_2$ process with different treatment time (0–60 min) is shown in Figure 4. The absorption peak at 400 nm mainly contributed to the formation of *p*-nitrophenolate ions in alkaline condition (Bae *et al.* 2015). The figure shows that the peaks of PNP at 400 nm decreased quickly with the ozonation reaction proceeding, and disappeared at treatment time of 20 min and longer, which indicated that the $-NO_2$ on the molecular structure of PNP was degraded effectively by $O_3/Ca(OH)_2$ system (Wan *et al.* 2017); at the same time, some new small peaks appeared at 200–300 nm with increasing reaction time. However, the absorbance intensity of the peaks at the range of 200–300 nm almost disappeared after 25–30 min treatment, which indicated that PNP in solution was almost mineralized completely, resulting in its high TOC removal efficiency. The

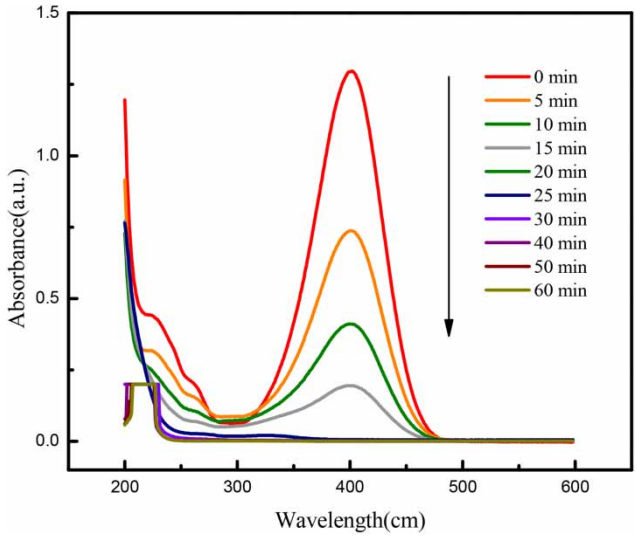

Figure 4 | UV-vis analysis of PNP under the optimum reaction conditions.

results of the UV-vis analysis were consistent with the variation of degradation and mineralization.

In order to further identify degradation intermediates of PNP and their variation by $O_3/Ca(OH)_2$ process, the intermediates in the three experiments contrasting the bubble system, microbubble system and $O_3/Ca(OH)_2$ system were analyzed by GC-MS analysis as shown in Figure S6. To confirm the structure of intermediate products, Figure S7 shows the chromatogram of intermediates of PNP degradation after reaction time of 20 min and 40 min in the bubble reactor (Figures S6 and S7 are available online).

As seen in Figure 5, there are some of the same intermediate products obtained by the three different processes. Several organic compounds, including 1,4-cyclohexanedione, 2-propanone,2-(1-methylethylidene) hydrazone, pentane, 2,2,3-trimethyl and 1-hexene-2,4-dimethyl-, were removed from the microbubble reactor. It is attributed to the effect of the microbubble rector. Otherwise, it is observed that the organic compounds in the $O_3/Ca(OH)_2$ process were less than half of those in microbubble process: only isopropyl cyclopropane carboxylate, butane, 2,2′-oxybis-, Ethyl butyrate and ethyl butyrate remained in the solution and mineralized completely after 60 min treatment. However, hydroquinone, detected in the bubble process and microbubble process, was not found in the $O_3/Ca(OH)_2$ process, which suggests that the ozonation process was accelerated by the addition of $Ca(OH)_2$; in other words, PNP could be oxidized into small molecules in a short period of time by the $O_3/Ca(OH)_2$ process. In addition, for example, isopropyl cyclopropane carboxylate was detected in 40–60 min ozonation treatment by microbubble process,

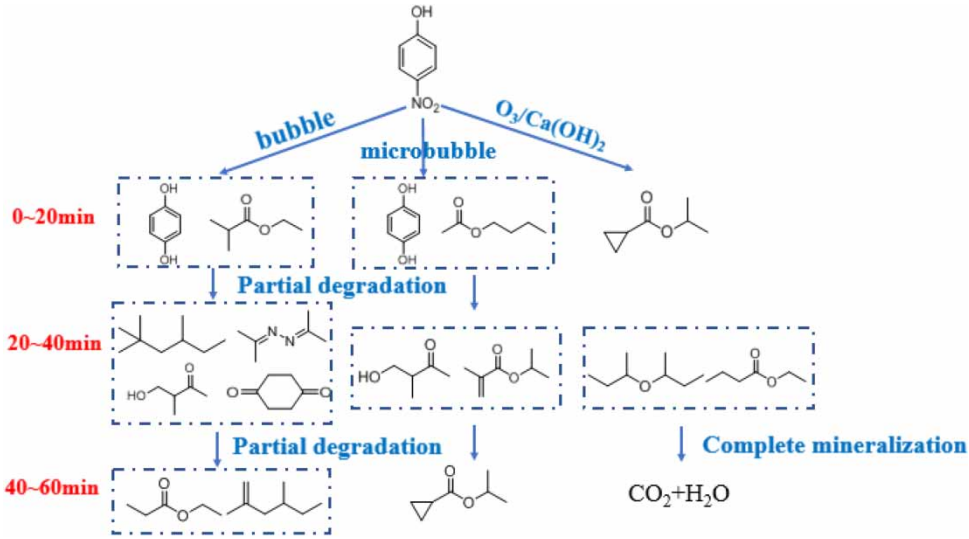

Figure 5 | The intermediate products of PNP degradation in the reaction process.

while it was detected in 0–20 min ozonation treatment in the presence of $Ca(OH)_2$. The chromatogram of intermediates of PNP degradation of reaction time 20 min and 40 min in the bubble reactor are shown in Figure S7. These results demonstrate that $Ca(OH)_2$ could facilitate ozone decomposition effectively and generate hydroxyl radical, thus accelerating the reaction rate and increasing the TOC removal efficiency.

Solid products analysis

The structures and crystallinity of solid products in the ozonation process were studied by XRD and the results are depicted in Figure 6. It can be seen that the crystalline product mainly including calcium hydroxide ($Ca(OH)_2$), calcium carbonate ($CaCO_3$), and calcium oxalate (CaC_2O_4). The new solid phase products were produced in the ozonation treatment from 0 min to 60 min, and it can be explained from the following two aspects. (i) The precipitation was formed between the direct oxidation by-products and calcium, such as calcium oxalate. In ozonation, ozone molecules attack PNP molecules, causing the partial degradation of PNP and forming some intermediates, such as fumaric acid, maleic acid, acrylic acid, and oxalate (Bakheet *et al.* 2013); this result is in accordance with the decrease of the pH in liquid phase in Figure 3. (ii) CO_3^{2-} ions were generated by the production of CO_2 in alkaline condition because of the mineralization of organic pollutants, forming the precipitation of $CaCO_3$.

As seen in Figure 6(a), the diffraction of $Ca(OH)_2$ disappeared gradually with prolonging of the ozonation time, illustrating that the Ca^{2+} ions and OH^- ion were consumed. Diffraction peaks assigned to calcium oxalate at

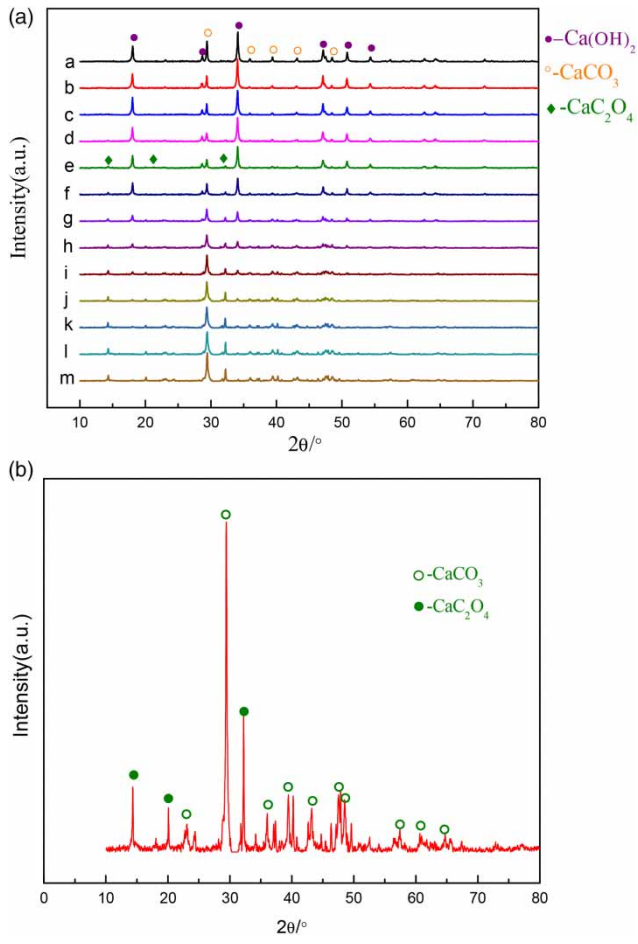

Figure 6 | The XRD analysis of the precipitated substances in $O_3/Ca(OH)_2$ system: a, 0 min; b, 5 min; c, 10 min; d, 15 min; e, 20 min; f, 25 min; g, 30 min; h, 35 min; i, 40 min; j, 45 min; k, 50 min; l, 55 min; m, 60 min (a). The diffraction pattern of the precipitated substances in 60 min (b).

$2\theta = 14.3°$, 20.1° and 32.24° appear at 20 min ozonation treatment. When PNP degraded into small molecular organics completely, it is indicated that oxalic acid in solution combined with calcium ions, forming precipitation of calcium oxalate that was detected in the XRD pattern. Also, diffraction peaks of calcium carbonate at $2\theta = 29.44°$, 35.94°, 39.4° and 47.68° exist in the precipitation and strengthen gradually. And Figure 6(b) displays the diffraction peak of the precipitated substances including CaC_2O_4 and $CaCO_3$.

To further research the surface properties, the surface characteristics of solid products after 60 min treatment were observed by SEM and FTIR as shown in Figure 7. Figure 7(a) shows the surface morphology of solid substances, some of which have a cube structure, which is a common calcite, and one of the most stable crystalline structures of calcium carbonate. Some have an irregular-shaped polygonal structure with rough surfaces and particles attached to crystals. It agrees with the structure of calcium oxalate.

Figure 7(b) shows the FTIR absorption spectrum of solid substance after PNP mineralization. The band at 3,447 cm^{-1} is attributed to the O-H stretching vibration; the absorption peak of OH is likely to come from the COOH, alcohol or phenol (Naushad *et al.* 2017). The band at 2,964 cm^{-1} is attributed to the $-CH_3$ antisymmetric

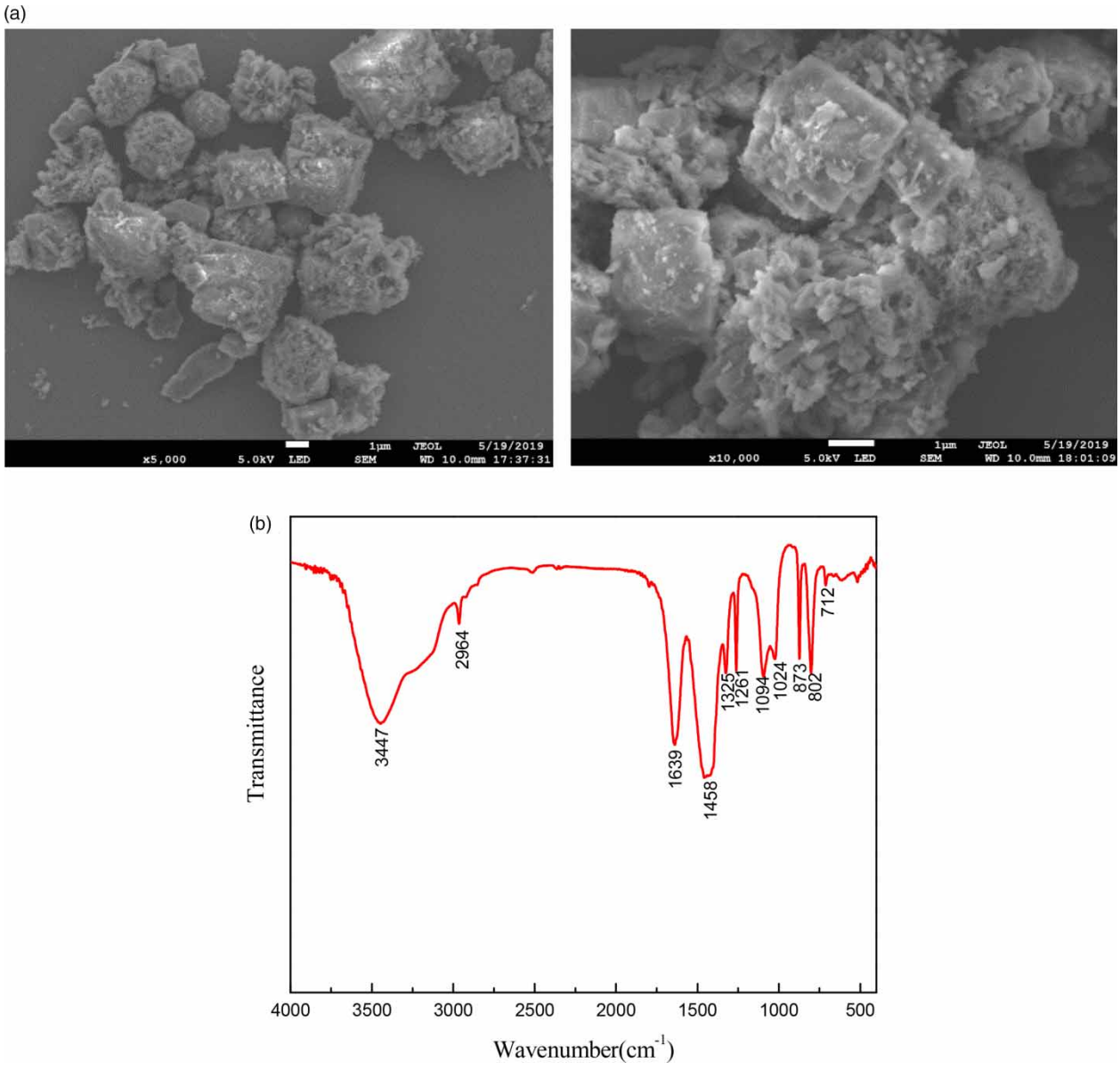

Figure 7 | The surface characteristics of solid substances after $O_3/Ca(OH)_2$ process: (a) SEM; (b) FTIR adsorption spectra of the 400–4000 cm^{-1} region.

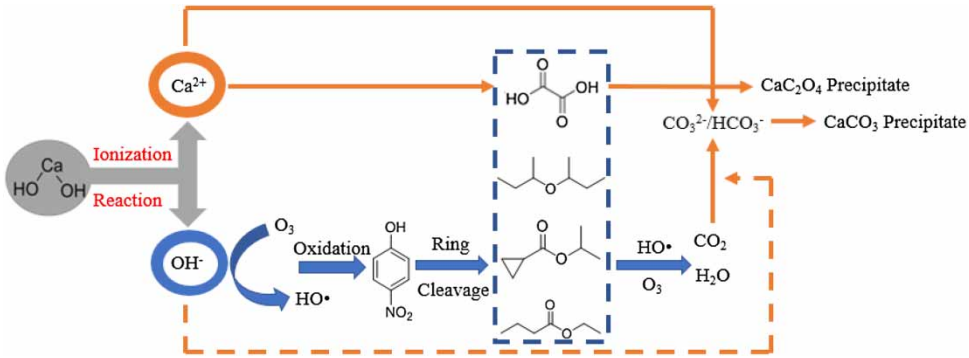

Figure 8 | The effect of $Ca(OH)_2$ in the ozonation process.

stretching vibration. The band at 1,639 cm^{-1} is attributed to the double band stretching vibration. The bands at 1,024, 1,094, 1,261, 1,325, and 1,458 cm^{-1} are attributed to the C-O stretching vibration, including carbohydrates, esters, ethers, which illustrates that COO- is generated by organic matter degradation (Albadarin *et al.* 2016). And the band at 873 cm^{-1} is attributed to the CO_3^{2-} out-of-plane deformation vibration; the band at 712 cm^{-1} is attributed to O-C-O in-plane deformation vibration. The characteristic absorption peaks of CO_3^{2-} and COO^- in IR spectrums verified the production of calcium oxalate and calcium carbonate.

In the O_3/$Ca(OH)_2$ process, the pH value of solution kept to 12.47 and reached saturation, which facilitates the effect of OH^- for the ozone decomposition and generation of hydroxyl radical. This verified that the oxalic acid and CO_3^{2-} ions were precipitated by the Ca^{2+} ions in the O_3/$Ca(OH)_2$ system, and this should be the mechanism of $Ca(OH)_2$-intensified mineralization of PNP solution. The whole mechanism could be summarized as Figure 8.

CONCLUSIONS

The ozonation of PNP by O_3/$Ca(OH)_2$ process in a microbubble reactor was discussed. PNP could be removed and mineralized efficiently in the presence of 3 g/L $Ca(OH)_2$. After 60 min treatment, the organic matter was almost mineralized completely, and the mineralization rate also was much higher than those of the O_3 process of 55.63% and $Ca(OH)_2$ process of 3.53% under certain conditions, which confirmed the superiority of the O_3/$Ca(OH)_2$ process. The removal rate increased with increasing ozone concentration up to 75 mg/L, ozone flow rate and 4 L/min, and decreasing initial PNP concentration; in addition, it was insignificantly affected by the external pressure and temperature.

$Ca(OH)_2$ combined with ozone could intensify the ozonation process, and the mechanism was explored through GC-MS analysis of the liquid samples and characterization analysis of the precipitated substances. The results show that the microbubble process improves the utilization of ozone, reducing the types of organic matter of PNP degradation compared to the bubble process, and the O_3/$Ca(OH)_2$ process could maintain the pH value in solution, accelerating the generation of hydroxyl radical, and thus leading to PNP being completely mineralized. Furthermore, the ozonation efficiency can be intensified by *in situ* precipitation and separation of hydroxyl radical scavengers and the intermediate product oxalic acid.

ACKNOWLEDGEMENTS

This work was supported by the National Science Foundation of China (grant number 21176273); the personnel project of Chongqing Science and Technology Committee (grant number 2014); and Chong Qing Municipal Solid Waste Resource Utilization & Treatment Collaborative Innovation Center.

REFERENCES

Al-Abduly, A., Christensen, P., Harvey, A. & Zahng, K. 2014 Characterization and optimization of an oscillatory baffled reactor (OBR) for ozone-water mass transfer. *Chemical Engineering and Processing: Process Intensification* **84**, 82–89.

Albadarin, A. B., Collins, M. N., Naushad, M., Shirazian, S. & Mangwandi, C. 2016 Activated lignin–chitosan extruded blends for efficient adsorption of methylene blue. *Chemical Engineering Journal* **307**, 264–272.

Al-Kahtani, A. A., Almuqati, T., Alhokbany, N., Naushad, M. & Alshehri, S. M. 2018 A clean approach for the reduction of

hazardous 4-nitrophenol using gold nanoparticles decorated multiwalled carbon nanotubes. *Journal of Cleaner Production* **191**, 429–435.

Alshehri, S. M., Naushad, M., Ahamad, T., Alothman, Z. A. & Aldalbahi, A. 2014 Synthesis, characterization of curcumin based ecofriendly antimicrobial bio-adsorbent for the removal of phenol from aqueous medium. *Chemical Engineering Journal* **254**, 181–189.

Asgari, G., Seid Mohammadi, A., Mortazavi, S. B. & Ramavandi, B. 2013 Investigation on the pyrolysis of cow bone as a catalyst for ozone aqueous decomposition: kinetic approach. *Journal of Analytical and Applied Pyrolysis* **99**, 149–154.

Bae, S., Gim, S., Kim, H. & Hanna, K. 2015 Effect of $NaBH_4$ on properties of nanoscale zero-valent iron and its catalytic activity for reduction of *p*-nitrophenol. *Applied Catalysis B: Environmental* **182**, 541–549.

Bakheet, B., Yuan, S., Li, Z., Wang, H., Zuo, J. & Komarneni, S. 2013 Electro-peroxone treatment of orange II dye wastewater. *Water Research* **47** (16), 6234–6243.

Bauman, M., Lobnik, A. & Hribernik, A. 2011 Decolorization and modeling of synthetic wastewater using O_3 and H_2O_2/O_3 processes. *Ozone: Science & Engineering* **33** (1), 8.

Cheng, M., Zeng, G., Huang, D., Lai, C., Xu, P. & Zhang, C. 2016 Hydroxyl radicals based advanced oxidation processes (AOPs) for remediation of soils contaminated with organic compounds: a review. *Chemical Engineering Journal* **284**, 582–598.

Derikvandi, H. & Nezamzadeh-Ejhieh, A. 2017 Increased photocatalytic activity of NiO and ZnO in photodegradation of a model drug aqueous solution: effect of coupling, supporting, particles size and calcination temperature. *Journal of Hazardous Materials* **321**, 629–638.

Hu, E., Shang, S., Tao, X. M., Jiang, S. & Chiu, K. L. 2016 Regeneration and reuse of highly polluting textile dyeing effluents through catalytic ozonation with carbon aerogel catalysts. *Journal of Cleaner Production* **137**, 1055–1065.

Izadifard, M., Achari, G. & Langford, C. H. 2018 Mineralization of sulfolane in aqueous solutions by ozone/CaO_2, and ozone/CaO with potential for field application. *Chemosphere* **197**, 535–540.

Khodami, Z. & Nezamzadeh-Ejhieh, A. 2015 Investigation of photocatalytic effect of ZnO–SnO_2/nano clinoptilolite system in the photodegradation of aqueous mixture of 4-methylbenzoic acid/2-chloro-5-nitrobenzoic acid. *Journal of Molecular Catalysis A: Chemical* **409**, 59–68.

Kumar, A., Naushad, M., Rana, A., Inamuddin, Preeti, Sharma, G., Ghfar, A. A., Stadler, F. J. & Khan, M. R. 2017 ZnSe-WO_3 nano-hetero-assembly stacked on Gum Ghatti for photo-degradative removal of bisphenol A: symbiose of adsorption and photocatalysis. *International Journal of Biological Macromolecules* **104**, 1172–1184.

Kuosa, M., Kallas, J. & Häkkinen, A. 2015 Ozonation of *p*-nitrophenol at different pH values of water and the influence of radicals at acidic conditions. *Journal of Environmental Chemical Engineering* **3** (1), 325–332.

Li, J., Liu, Q. & Ji, Q. Q. 2017 Degradation of *p*-nitrophenol (PNP) in aqueous solution by Fe^0-PM-PS system through response surface methodology (RSM). *Applied Catalysis B Environmental* **200**, 633–646.

Lu, S. & Pei, L. 2016 A study on phenol migration by coupling the liquid membrane in the ionic liquid. *International Journal of Hydrogen Energy* **41** (35), 15724–15732.

Mahyar, A., Miessner, H., Mueller, S. & Moeller, D. 2017 Empirical determination and modeling of ozone mass transfer in a planar falling film reactor. *Chemical Engineering Research and Design* **121**, 287–294.

Naushad, M., Ahamad, T., Al-Maswari, B. M., Alqadami, A. B. & Alshehri, S. M. 2017 Nickel ferrite bearing nitrogen-doped mesoporous carbon as efficient adsorbent for the removal of highly toxic metal ion from aqueous medium. *Chemical Engineering Journal* **330**, 1351–1360.

Nawrocki, J. & Kasprzyk-Hordern, B. 2010 The efficiency and mechanisms of catalytic ozonation. *Applied Catalysis B Environmental* **99** (1), 27–42.

Nezamzadeh-Ejhieh, A. & Ghanbari-Mobarakeh, Z. 2015 Heterogeneous photodegradation of 2,4-dichlorophenol using FeO doped onto nano-particles of zeolite P. *Journal of Industrial and Engineering Chemistry* **21**, 668–676.

Nezamzadeh-Ejhieh, A. & Khorsandi, M. 2010 Heterogeneous photodecolorization of Eriochrome Black T using Ni/P zeolite catalyst. *Desalination* **262** (1–3), 79–85.

Quan, X., Luo, D., Wu, J., Li, R., Cheng, W. & Ge, S. 2017 Ozonation of acid red 18 wastewater using O_3/Ca(OH)$_2$ system in a micro bubble gas-liquid reactor. *Journal of Environmental Chemical Engineering* **5** (1), 283–291.

Rischbieter, E., Stein, H. & Schumpe, A. 2000 Ozone solubilities in water and aqueous salt solutions. *Journal of Chemical & Engineering Data* **45** (2), 338–340.

Senobari, S. & Nezamzadeh-Ejhieh, A. 2018 A comprehensive study on the enhanced photocatalytic activity of CuO-NiO nanoparticles: designing the experiments. *Journal of Molecular Liquids* **261**, 208–217.

Shahidi, D., Roy, R. & Azzouz, A. 2015 Advances in catalytic oxidation of organic pollutants – prospects for thorough mineralization by natural clay catalysts. *Applied Catalysis B: Environmental* **174–175**, 277–292.

Takahashi, M., Ishikawa, H., Asano, T. & Horibe, H. 2012 Effect of microbubbles on ozonized water for photoresist removal. *Journal of Physical Chemistry C* **116** (23), 12578–12583.

Wan, D., Li, W., Wang, G., Lu, L. & Wei, X. 2017 Degradation of *p*-nitrophenol using magnetic Fe(0)/Fe_3O_4/coke composite as a heterogeneous Fenton-like catalyst. *Science of the Total Environment* **574**, 1326–1334.

Wang, J. & Bai, Z. 2016 Fe-based catalysts for heterogeneous catalytic ozonation of emerging contaminants in water and wastewater. *Chemical Engineering Journal* **312**, 79–98.

Wang, T., Qu, G., Sun, Q., Liang, D. & Hu, S. 2015 Evaluation of the potential of *p*-nitrophenol degradation in dredged sediment by pulsed discharge plasma. *Water Research* **84**, 18–24.

Wang, Y., Yang, W., Yin, X. & Liu, Y. 2016 The role of Mn-doping for catalytic ozonation of phenol using Mn/γ-Al_2O_3 nanocatalyst: performance and mechanism. *Journal of Environmental Chemical Engineering* **4** (3), 3415–3425.

Xiong, Z., Lai, B., Yuan, Y., Cao, J., Yang, P. & Zhou, Y. 2016 Degradation of *p*-nitrophenol (PNP) in aqueous solution by a micro-size Fe^0/O_3 process (mFe^0/O_3): optimization, kinetic, performance and mechanism. *Chemical Engineering Journal* **302**, 137–145.

Yu, S., Hu, J. & Wang, J. 2011 Gamma radiation-induced degradation of *p*-nitrophenol (PNP) in the presence of hydrogen peroxide (H_2O_2) in aqueous solution. *Acta Scientiae Circumstantiae* **177** (1), 1061–1067.

Zhang, X., Feng, M., Qu, R., Hui, L., Wang, L. & Wang, Z. 2016 Catalytic degradation of diethyl phthalate in aqueous solution by persulfate activated with nano-scaled magnetic $CuFe_2O_4$/MWCNTs. *Chemical Engineering Journal* **301**, 1–11.

Zeng, Z., Zou, H., Li, X., Sun, B., Chen, J. & Shao, L. 2012 Ozonation of acidic phenol wastewater with O_3/Fe(II) in a rotating packed bed reactor: optimization by response surface methodology. *Chemical Engineering and Processing: Process Intensification* **60** (10), 1–8.

First received 18 February 2019; accepted in revised form 24 June 2019. Available online 2 July 2019